Methods and Applications in Fluorescence

Comparison of MSD analysis from single particle tracking with MSD from images. Getting the best of both worlds

To cite this article before publication: Constanza Kettmayer *et al* 2023 *Methods Appl. Fluoresc.* in press https://doi.org/10.1088/2050-6120/acfd7e

Comparison of MSD analysis from single-particle tracking with MSD from images. Getting the best of both worlds

Constanza Kettmayer[1,2], Enrico Gratton[3], and Laura C. Estrada *[1,2]

[1] *Universidad de Buenos Aires, Facultad de Ciencias Exactas y Naturales, Departamento de Física. Buenos Aires, Argentina*

[2] *CONICET - Universidad de Buenos Aires, Instituto de Física de Buenos Aires (IFIBA). Buenos Aires, Argentina*

[3] *Laboratory for Fluorescence Dynamics, Biomedical Engineering Department, University of California, Irvine, CA, USA.*

Abstract

Fluorescence microscopy can provide valuable information about cell interior dynamics. Particularly, mean squared displacement (MSD) analysis is widely used to characterize proteins and sub-cellular structures' mobility providing the laws of molecular diffusion. The MSD curve is traditionally extracted from individual trajectories recorded by single-particle tracking-based techniques. More recently, image correlation methods like iMSD have been shown capable of providing averaged dynamic information directly from images, without the need for isolation and localization of individual particles. iMSD is a powerful technique that has been successfully applied to many different biological problems, over a wide spatial and temporal scales. The aim of this work is to review and compare these two well-established methodologies and their performance in different situations, to give an insight on how to make the most out of their unique characteristics. We show the analysis of the same datasets by the two methods. Regardless of the experimental differences in the input data for MSD or iMSD analysis, our results show that the two approaches can address equivalent questions for free diffusing systems. We focused on studying a range of diffusion coefficients between D = 0.001 $\mu m^2/s$ and D = 0.1 $\mu m^2/s$, where we verified that the equivalence is maintained even for the case of isolated particles. This opens new opportunities for studying intracellular dynamics using equipment commonly available in any biophysical laboratory.

1 Introduction

Fluorescence microscopy has long been an essential tool in biological research. Due to its high sensitivity and specificity, along with the possibility of applying it to living cells in a minimally invasive way, it is widely used to visualize and analyze complex intracellular dynamic events as they occur [1–3]. In particular, studying quantitatively the mobility of proteins and subcellular structures can yield valuable information about their functions [4–6].

In this context, single-particle tracking (SPT) is a powerful approach to evaluating the diffusive motion of biomolecules. In contrast with more traditional bulk methods like fluorescence recovery after photobleaching (FRAP) [7], which averages over hundreds of diffusing molecules, SPT measures individual trajectories, providing high specificity [8]. By computing the mean-square displacement (MSD) from trajectories, SPT can resolve the modes of motion of individual molecules. However, one of the main drawbacks of this technique is the need for a large number of trajectories to be recorded to improve the statistical significance of the results.

An attractive alternative that overcomes some of the SPT limitations can be found in spatiotemporal image correlation spectroscopy (STICS) [9] and image-derived mean squared displacement (iMSD) [10]. These methods can evaluate modes of motion by analyzing the time dependence of the fluorescence intensity correlation in a stack of images, without the need for localization. These properties make iMSD a powerful technique for studying relevant biological problems, such as the diverse intracellular

*lestrada@df.uba.ar

dynamic processes and the viscosity of the cell interior [6, 10–17]. As with any other fluctuation-based analysis method, iMSD provides average information about all the diffusing elements in the image stack, allowing good statistics in a limited amount of time [10].

iMSD also provides a conclusive analysis of the nature of the translational motion in the cell interior, by measuring protein mobility at the spatial and temporal nanoscale with no *a priori* assumptions on their diffusion properties [11]. iMSD has been successfully used to probe the molecular diffusion of an inert, fluorescent protein probe (GFP) in the intracellular environment in a variable timescale, from 1 μs to 100 μs [11]. This approach unveiled unobstructed Brownian motion from 25 to 100 nm and partially suppressed diffusion above 100 nm, which has been attributed to the presence of immobile and spatially-organized intracellular structures, rather than to diffusing crowding agents [11].

In this article, we apply the two approaches to the same synthetic datasets, to compare the results and discuss the advantages and limitations of both methods.

1.1 Theory

1.1.1 Mean squared displacement analysis from trajectories

Mean squared displacement (MSD) analysis is a robust tool widely used to characterize single-particle trajectories and quantitatively determine several dynamic parameters [18–20]. For a single-particle trajectory composed of a series of n particle positions observed at specific times t, the MSD can be computed for time lags $\tau = n$t according to

$$MSD(n) = \frac{1}{N-n}\sum_{i=1}^{N-n}(r_{i+n} - r_i)^2, \tag{1}$$

defined here for a trajectory r(t) of total length N, recorded at sampling time-intervals t. For a 2-dimensional diffusion process, the MSD generally scales with a power law according to

$$MSD(\tau) = 4D\tau^{\alpha}, \tag{2}$$

where D is the diffusion coefficient and α is the anomalous parameter. In the case of Brownian motion $\alpha = 1$ and the analytical expression is reduced to

$$MSD(\tau) = 4D\tau, \tag{3}$$

For $\alpha \neq 1$, the power law describes a process generally called anomalous diffusion, which can be categorized as superdiffusive ($\alpha > 1$), as in the case of active transport, or subdiffusive ($\alpha < 1$), as the case of diffusion in a crowded environment [8].

The free diffusion model is characteristic of unrestricted stochastic particle motion, active transport may result from molecular motor-driven processes and subdiffusive behavior can be the product of interaction with local obstacles and barriers, abundant in complex highly crowded environments like the cell interior. In reality, more than one process often occurs together, yielding more complex motion models described by linear combinations of the above expressions.

The main individual processes undergoing pure diffusion mechanisms are schematically shown in Fig. 1. By plotting the MSD curve and fitting it with these models, an MSD analysis can extract the law of diffusion that best describes the particle 2D motion.

1.1.2 Imaging derived mean squared displacement analysis

Recent works have shown that mean squared displacement can also be obtained directly from imaging without resolving the specific single-particle trajectories [6, 10, 12–17]. iMSD computes the spatiotemporal correlation function for increasing lag times τ in an image series, using the same mathematical basis of the STICS method [9]. The spatiotemporal correlation function can be defined as:

$$g(\xi,\eta,\tau) = \frac{\langle I(x,y,t)\cdot I(x+\xi,y+\eta,t+\tau)\rangle}{\langle I(x,y,t)\rangle^2} - 1, \tag{4}$$

where I represents fluorescence intensity, ξ and η are the distance between correlated pixels in x and y directions, and $\langle ...\rangle$ indicates the average over x, y and t variables.

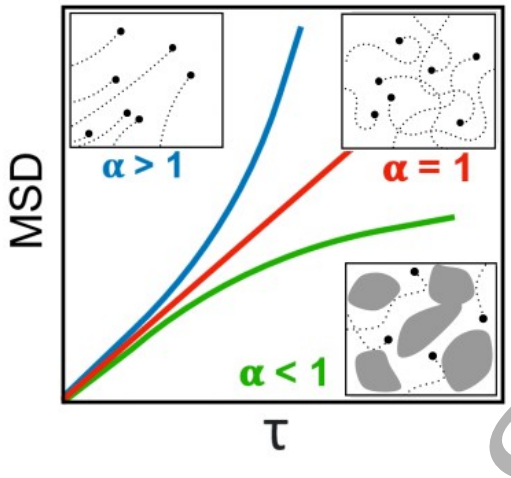

Figure 1: MSD curves for normal diffusion (red), superdiffusion (blue), and subdiffusion (green), as described by Eq. (2). Some biologically relevant examples of these situations are Brownian motion, directed motion and diffusion in a highly crowded environment, respectively.

If particles are diffusing, the width of the correlation central peak increases with τ. This increment is intrinsically connected to the average rate and mode of diffusion. Correlation peaks are then fitted by the Gaussian function:

$$G(\xi,\eta,\tau) = \frac{\gamma}{N\pi\sigma^2(\tau)} exp\left(-\frac{\xi^2+\eta^2}{\sigma^2(\tau)}\right), \tag{5}$$

where γ is a factor associated with observation volume shape, N is the average number of particles in the observation volume and the variance σ^2 represents the MSD. Thanks to the σ^2 vs. τ plot, that we will refer to as the iMSD curve, diffusion modes can be directly identified by using the already described mathematical framework for MSD [10].

In addition, iMSD analysis provides an estimation of the average diffusing particle size, through the offset of the iMSD curve (σ_0^2). The difference between σ_0^2 and the independently measured instrumental waist yields the particle size [10].

2 Materials and methods

2.1 Simulations and synthetic images generation

To evaluate the performance of the MSD and iMSD analysis in a controlled setting, we applied them to synthetic images of point-like particles undergoing Brownian motion in a 2D plane. Simulating 2D systems allowed us to ensure a direct comparison by using the same set of data images to apply iMSD and also to track single-particles during the same time interval (as particles can not leave the focal plane). Since the iMSD method is always applied to image series, where the acquisition is restricted to the focal plane components of movement, conclusions derived from this analysis can be extrapolated to 3D systems. The simulations were performed using a commercial closed-source software SimFCS (LFD, University of California, Irvine, available at https://www.lfd.uci.edu/globals/).

In the simulations, particles are randomly seeded in a 2D square grid with periodic boundaries. One unit of the grid is equal to 50 nm, and the total size is 256 × 256 units. Particles move in the grid according to given rules of diffusion. To achieve this, at each step of the simulation the routine calculates the probability to move a particle in each possible direction, depending on the diffusion coefficient of the particle. Then, the position of each particle and the given point spread function (PSF) are used to calculate the total intensity of the particle, and the Poisson statistics are applied to simulate the statistics of photons. Brightness was set as 10^6 counts per second per particle. Additionally, a background noise of 100 counts per second with a Poisson distribution was added in the simulated images. All synthetic datasets were 256 × 256 at a resolution of 50 nm/pixels, and 1000

frames long with a time step of 10 ms/frame. The simulation frame rate was chosen to be similar to those obtained in commercial cameras typically used in biophysics laboratories. The PSF was set in a 3D Gaussian shape with a 300 nm waist in the radial direction.

2.2 Tracking and MSD analysis software

Particle trajectories were captured from synthetic image datasets using the SpotTracker add-on with ImageJ [21]. This software can extract the optimal space-time trajectory (x, y, t) of a given particle by applying a dynamic programming optimization procedure. We chose this tracker as this is a free add-on to ImageJ, a public domain image processing software, widely used for biophysics applications.

Then the MSDs for each trajectory were calculated using a custom-made Python script. The script uses Eq. (1) to compute an MSD curve, which is then fit to different diffusion models and the R^2 value is calculated. This allows the script to determine which of the models is a better fit for the system and then calculate the corresponding movement parameters.

iMSD processing and the subsequent data analysis were performed with an iMSD script working in MATLAB (MathWorks Inc., Natick, MA.) described in [16].

3 Results

3.1 MSD from trajectories

To test and compare the accuracy of MSD analysis when it is computed from tracked trajectories and when it is extracted directly from images, in this section we will perform both analysis on the same dataset to compare the obtained results. First, we will show an example of tracking and MSD analysis by studying the motion of single-particles in a synthetic image dataset. The dataset corresponds to a free diffusion simulated system of 30 particles, with a diffusion coefficient of 0.01 $\mu m^2/s$. We chose a particle that remained far enough from the rest to be able to identify it at all times. This is important to ensure that we are always tracking the same particle, and not hopping between close particles. An example frame of this dataset is shown in Fig. 2 (a). Then we used the ImageJ plugin to record its trajectory, which is displayed in Fig. 2 (b). The trajectory is conformed by 500 data points and corresponds to an elapsed time of 5 s which is indicated by the described color code, where blue corresponds to the start of the trajectory and yellow to its end. From these data, we calculated the mean squared displacements using our Python script and obtained the MSD curve shown in Fig. 2 (c). The obtained MSD curve exhibits a linear trend, consistent with the simulated diffusive motion. We then fitted the MSD curve with the Brownian model (Eq. (3)) and estimated a diffusion coefficient of $(9.57 \pm 0.06)\ 10^{-3}\ \mu m^2/s$, different from the simulated value in less than 5%.

If we are interested in the average dynamics of the system, it is necessary to record and analyze several trajectories to increase the statistical significance of the estimated mean diffusion coefficient. In Fig. 3 (a) we show the result of tracking 10 different particles in the same dataset and independently analyze these trajectories by MSD. As a result, we have 10 different MSD curves that exhibit a similar linear trend, where each of them represents the dynamics of a single-particle. Then, we averaged these curves for each lag time τ, obtaining a mean MSD curve. This curve provides information on the average motion of the system, and the fit by the Brownian model yields a mean diffusion coefficient of $(9.42 \pm 0.04)\ 10^{-3}\ \mu m^2/s$. Even when there is a dispersion in the estimated diffusion coefficients for single-particles, each of them can differ up to 30% from the simulated value, and the mean diffusion coefficient well agrees with the performed simulation. It is important to note that this deviation from the simulated value for individual particles does not imply a lack of accuracy in the analysis. Due to the inherent randomness of the diffusion process, each simulated particle follows a distinct trajectory, and individual diffusion coefficients measured over finite time periods may exhibit variability.

3.2 MSD from imaging

The MSD curve can also be directly extracted from imaging, with no need to extract and analyze individual single-particle traces, by analyzing the spatiotemporal correlation with STICS [10]. To compare both methods, we re-analyzed the same dataset by iMSD. This provided the iMSD curve displayed in Fig. 3 (b), which exhibits an expected linear trend. By fitting this curve with the Brownian model, we calculated a diffusion coefficient of $(9.57 \pm 0.01)\ 10^{-3}\ \mu m^2/s$.

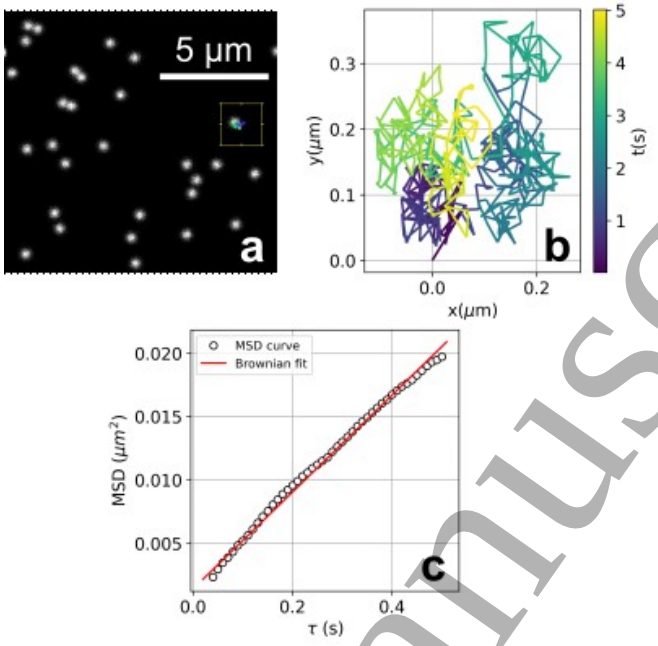

Figure 2: Tracking and MSD analysis results for computer-generated simulations. (a) Image from the synthetic dataset generated from the simulation of a system of 30 free diffusing particles with D = 10 $\times$ 10^{-3} $\mu m^2/s$. The square shows the representative particle that was selected to be tracked and the recorded trajectory. (b) Detail of the recorded trajectory. (c) MSD analysis from the trajectory and the fit with a Brownian model, which yields a diffusion coefficient of (9.57 $\pm$ 0.06) 10^{-3} $\mu m^2/s$ is also shown (solid red line).

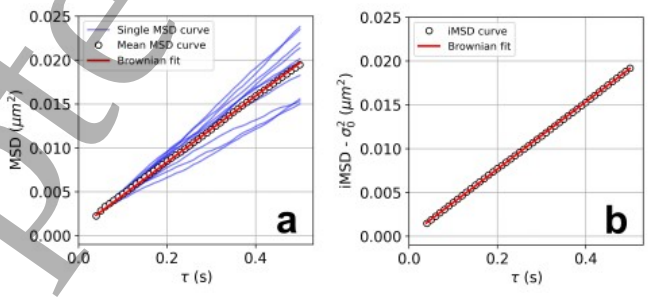

Figure 3: Mean squared displacement as a function of lag time τ. Analysis of average dynamics by MSD from tracking (Section 3.1) and iMSD (Section 3.2). (a) 10 single-particles trajectories were tracked and analyzed by MSD (blue), these curves were averaged for each time lag τ (black) and fitted by the Brownian model (red), which yielded a mean diffusion coefficient of (9.42 $\pm$ 0.04) 10^{-3} $\mu m^2/s$. (b) An equivalent analysis was performed using iMSD in the same dataset. The iMSD curve (black) was fitted by the Brownian model (red), giving a mean diffusion coefficient of (9.57 $\pm$ 0.01) 10^{-3} $\mu m^2/s$. For ease of comparison between both curves, the iMSD intercept value σ_0^2 was subtracted.

iMSD results reflect all information present in the image series and therefore provide a characterization of the average motion of the whole particle system. It is, therefore, reasonable to compare this result to the mean MSD curve in Fig. 3 (a). The diffusion coefficients estimated by the fitting of both curves are equally precise and differ by less than 2%. Proving that regardless of the experimental differences in the input data for both approaches (trajectories in one case, images in the other), they can provide completely equivalent information on the averaged dynamics of the system. This agreement in the results was verified for a series of simulations of free diffusing particles in a range between D = 0.001 $\mu m^2/s$ and D = 0.1 $\mu m^2/s$, maintaining the same simulation and analysis parameters (Supplementary Fig. 1).

In this sense, iMSD has the advantage of affording good statistics from only one measurement and analysis. By avoiding localizing single-particles, we can obtain robust results in a faster and more practical way. Additionally, iMSD provides quantitative information about the size of the particles under study. In this case particles are point-like, and therefore the intercept value on the Brownian fit σ_0^2 represents the squared instrumental waist. The recovered value from the fit was (305.98 ± 0.06) nm, which is consistent with the simulated 300 nm.

3.2.1 iMSD analysis and particle concentration

We have shown that iMSD analysis takes advantage of all information contained in the image series, providing a robust and fast characterization of the average motion. In this section, we interrogate the validity of this approach in two contrasting scenarios: one where the system under study has a very low concentration, and other where the concentration is too high for single particle tracking.

First we analyze the low concentration case. Specifically, we show results on the iMSD analysis of a single isolated particle. Even though the application of this method to this kind of system is in principle possible [16], it has not been experimentally validated. To evaluate these results, we study the same particle in two independent ways: by MSD from tracking and by iMSD from the image series. We chose a new particle in the same synthetic dataset, tracked it, and analyzed the trajectory by MSD. This is depicted in Fig. 4 (a,b,c). The results show diffusive motion with D = (6.72 ± 0.05) 10^{-3} $\mu m^2/s$, 30% lower than the simulated value. This is a particle with a slower motion than the system average.

We want to study the motion of this particle by iMSD, in a way that ensures that the analysis conditions remain the same. Since iMSD results describe the average motion of all particles in the image series, we subtracted all unwanted particles in every frame of the series (by replacing them with dark pixels) before applying iMSD (See Fig. 4 (d)). The method computed the spatiotemporal correlation function and the iMSD curve, shown in Fig. 4 (e, f). This yielded a diffusion coefficient for the particle of D = (6.51 ± 0.03) 10^{-3} $\mu m^2/s$, 30% lower than the simulated 10 × 10^{-3} $\mu m^2/s$. Again, we see a deviation from the average diffusion coefficient of the system. Both results differ by less than 4% and are equally precise, confirming that the equivalence between MSD from tracking and iMSD persists even for the case of single-particle motion, validating the application of iMSD in diluted samples.

On the other hand, we study a case of higher particle concentration. We maintained simulation and analysis parameters as described before, while increasing the number of simulated particles to test the potential impact in iMSD accuracy. In Fig. 5, we present a simulation of 4000 particles (corresponding to 24.41 particles/μm^2) exhibiting normal diffusion with D = 0.01 $\mu m^2/s$. This is an example of a system that would not be possible to be analyzed by SPT and MSD, due to the high proximity between particles. The iMSD analysis yielded a D value of (9.73 ± 0.05) 10^{-3} $\mu m^2/s$, which is consistent with the discrepancies observed for lower concentrations. This finding affirms that iMSD can be used in a broader range of concentration than SPT.

3.2.2 iMSD on two-population systems

We have seen that iMSD is a convenient approach to studying a set of isotropically diffusing particles, as it provides a precise quantitative description of the average motion. However, real biological applications usually involve much more complex systems, composed of more than one population with different dynamic properties. In this section we evaluate whether iMSD is capable of detecting the presence of multiple species with different dynamic behavior, and we examine what kind of information it can offer in such scenarios. The possibility of using fluctuation analysis approaches such as iMSD to

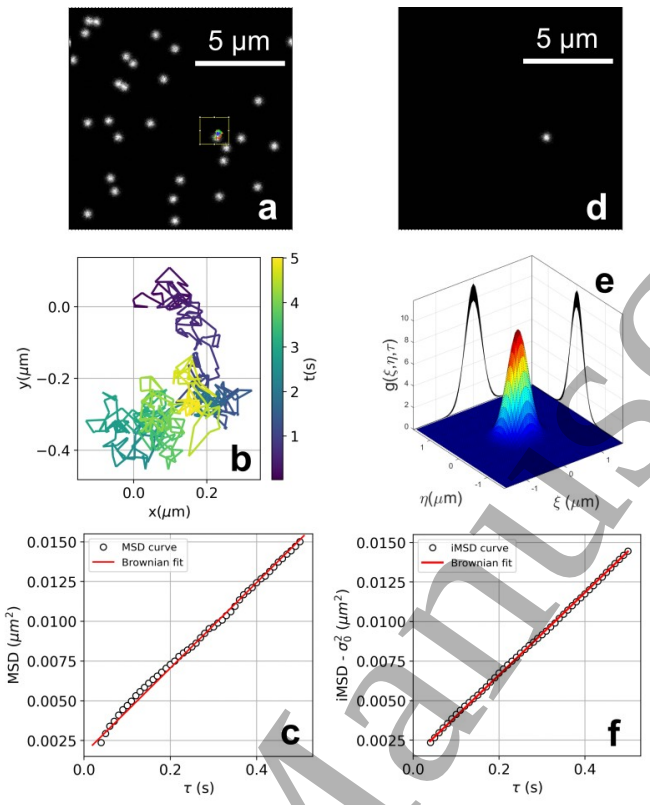

Figure 4: Analysis of a single-particle dynamics by two methods: MSD from tracking and iMSD. (a) Image from the synthetic dataset. The square shows the particle that was selected to be tracked and the recorded trajectory. (b) Detail of the recorded trajectory. (c) MSD analysis from the trajectory and Brownian fit, that yields a diffusion coefficient of D = (6.72 ± 0.05) 10^{-3} $\mu m^2/s$. (d) To study the same particle by iMSD we subtracted the rest of them from all the images of the series. (e) Spatiotemporal correlation function computed by the method. (f) iMSD curve and Brownian fit, which gives a diffusion coefficient of D = (6.51 ± 0.03) 10^{-3} $\mu m^2/s$. The consistency in both results validates the application of iMSD to low-concentration systems.

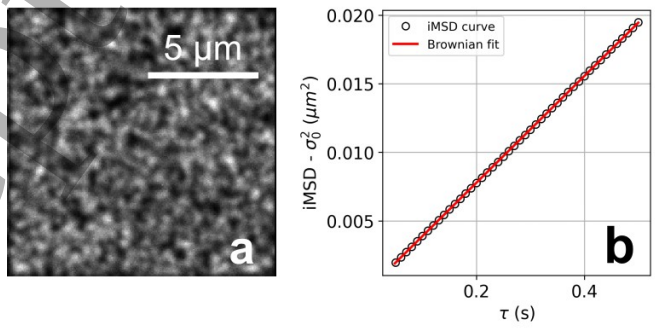

Figure 5: iMSD analysis of a simulation of 4000 particles (24.41 particles/μm^2) normally diffusing with D = 0.01 $\mu m^2/s$. (a) An illustrative frame extracted from the generated synthetic image series. (b) Fitting the iMSD curve with the Brownian model yielded a D value of (9.73 ± 0.05) 10^{-3} $\mu m^2/s$. This discrepancy is in agreement with results obtained for lower particle concentrations.

provide complementary results to single-particle tracking methods in this situation has not yet been explored deeply.

If these populations are localized in separate regions, an independent iMSD analysis of each of them can be achieved simply by choosing a smaller region of interest. We will focus on the case in which populations coexist in the same region in a random spatial distribution. We generated a new series of synthetic datasets from the simulation of the simplest scenario, in which two populations of 15 free diffusing particles with different diffusion coefficients are randomly seeded across the images. The rest of the simulation parameters were kept the same as in the previous sections.

In Fig. 6 (a) we present the iMSD analysis of one of these datasets, in which half of the particles move with $D_1 = 0.1\ \mu m^2/s$ and the other half with $D_2 = 0.002\ \mu m^2/s$. The iMSD curve does not show the linear tendency expected for diffusive motion. It differs from the straight lines predicted for D_1 and D_2 by the Brownian model, but also from the averaged $(D_1+D_2)/2$. Instead, it exhibits the typical curvature that characterizes the sub-diffusive regimen, and as such, it can be fitted by the anomalous diffusion model (Eq. (2)). This fit gives an anomalous diffusion parameter of $\alpha = 0.54 \pm 0.02$.

This shows that even if iMSD provides averaged information about the motion of the whole system, the analysis isn't blind to the presence of more than one population with different dynamics. The iMSD curve with $\alpha < 1$ indicates the existence of a difference in the system's average behavior at two spatiotemporal scales. At short time lags, the slower population has barely moved, and so the average motion predominately represents the faster population and the iMSD curve slope is higher. On the other hand, at long time lags, both populations are represented in the average motion, and the slope decreases.

This disparity increases with the ratio $R = D_1/D_2$. To study the effect of R in the parameter α, we varied the diffusion coefficients D_1 and D_2 generating a series of datasets with different ratios. Each of them was independently analyzed by iMSD and a value for α was estimated from the fitting of the curve by the anomalous diffusion model. Results are displayed in Fig. 6 (b), where each point represents a different dataset and the color code shows the estimated α. We can see that while the α value for points in the same R line is similar, higher R ratios can be associated with a lower α. This result suggests that the anomalous diffusion parameter, could serve as a qualitative indicator of the disparity of the populations' motion.

The proposed methodology is useful to detect the presence of more than one population of normally diffusing particles, and qualitatively characterize it. However, it should be noted that it fails to determine if the low anomalous parameter is the result of a mixture of this kind or if it is the product of true subdiffusion. To obtain a complete characterization of the different behaviors at the individual particle level, techniques like SPT should be used. However, iMSD can still be valuable as a highly accessible and fast method to complement SPT. For example, if iMSD yields $\alpha < 1$, tracking a small number of particles would differentiate subdiffusion from normal diffusion. In other cases, after tracking a small sample, iMSD provides fast average information that could support or disprove the generalization of the results to bigger systems. Also, prior information about the biological system such as expected level of interaction or variability in behavior can anticipate these results.

3.2.3 iMSD analysis and signal noise

In previous sections, iMSD analysis was applied to simulations of particles with a brightness of 10^6 counts per second per particle and a non-correlated background noise of 100 counts per second. In the case where on average only one particle is present in the observation volume at a time, this corresponds to a ratio between background and particle brightness of $R_B = 10^{-4}$. To test the performance of iMSD in less favorable conditions we repeated the analysis for different noise-to-particle brightness ratios, by increasing R_B.

We generated eight series of images using a Poisson distribution with a given brightness, ranging from 500 cps to 1 Mcps, and overlaid it onto a simulation of free-diffusing particles with a diffusion coefficient of $10 \times 10^{-3}\ \mu m^2/s$, as analyzed in Sections 3.1 and 3.2. We then applied the iMSD method to each overlap and compared the results for the obtained diffusion coefficient, ensuring that the analysis conditions remained constant thus any variation in the results could then be attributed to the presence of noise.

We found that by increasing background noise up to a ratio of $R_B = 0.2$ (i. e. particles five times brighter than background noise), we obtained a diffusion coefficient $D = (9.64 \pm 0.01)\ 10^{-3}$

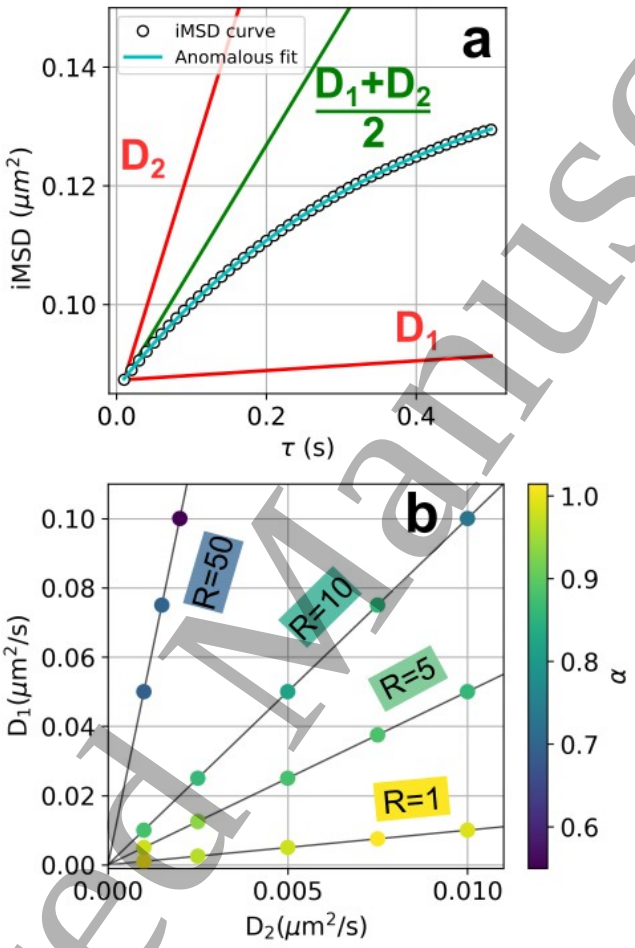

Figure 6: iMSD analysis of systems conformed by two species of free diffusing particles with different D coexisting in the same space. (a) iMSD curve for the case of $D_1 = 0.1\ \mu m^2/s$ and $D_2 = 0.002\ \mu m^2/s$ ($R = D_1 / D_2 = 50$). The curve is inconsistent with the straight lines predicted for D_1, D_2, or $(D_1+D_2)/2$ by the Brownian model (red and green). Instead, it exhibits the typical curvature of a subdiffusive motion, and anomalous fitting (Eq. (2)) yields a value of $\alpha = 0.54 \pm 0.02$. (b) Estimated α values for a set of systems consisting of two populations with different D_1 and D_2. Black straight lines highlight the points corresponding to the same ratio $R = D_1 / D_2$. Higher diffusion coefficient ratios, R, consistently result in a lower range of obtained α values, providing qualitative insights about the disparity of both populations' motion.

$\mu m^2/s$ (Fig. 7). This result differs by less than 1% from analyses with smaller R_B values. However, for simulations with higher backgrounds ($R_B \geq 0.3$), no correlation was detected, and a diffusion coefficient value could not be extracted from the analysis, even when the contrast in the image was high enough to distinguish particles from the background (Fig. 7 (c)). Based on these tests, we can identify a critical ratio of $R_B = 0.3$, that represents the lowest noise-to-particle brightness ratio at which iMSD analysis fails to produce reliable results. We replicated this analysis for four additional equivalent simulations, in which we corroborated the consistency of these findings. Simulations with $R_B = 0.2$ were accurately analyzed, obtaining the expected linear iMSD curves and diffusion coefficient values that always differed in less than 3% from those obtained in absence of significant noise. In contrast, no reliable analysis could be conducted for any of the simulations with $R_B = 0.3$ (Supplementary Fig. 2). We also analyzed the impact of a noise-to-particle brightness ratio of $R_B = 0.2$ on iMSD results for different particle brightness, obtaining consistent results (Supplementary Fig. 3).

We repeated this analysis for an isolated particle simulation presented in Section 3.2.1. In this case, we were able to obtain D values that differ by less than 1% for ratios within $R_B \leq 0.05$, while satisfactory results cannot be achieved for $R_B \geq 0.1$. We can thus determine a critical ratio of $R_B = 0.1$. As expected, the loss of correlation occurs at a smaller ratio than in the previous case, indicating that iMSD results are more sensitive to the presence of noise on diluted samples, where information available for computation is limited.

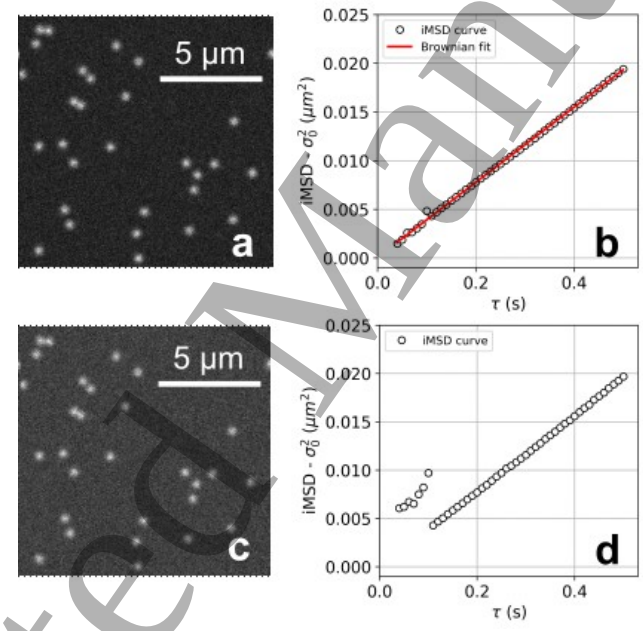

Figure 7: iMSD analysis of simulated free diffusing particles with $D = 10 \times 10^{-3}$ $\mu m^2/s$ for different brightness of the background Poissonian noise. (a) Simulation with a background-particle brightness ratio of $R_B = 0.2$. (b) iMSD analysis provided a result of $D = (9.64 \pm 0.01)\ 10^{-3}$ $\mu m^2/s$. This value differs by less than 1% for every $R_B \leq 0.2$. (c) Simulation with a background-particle brightness ratio of $R_B = 0.3$. (d) For this and bigger ratios, the noise causes correlation to be lost and a value of D can not be extracted from the iMSD analysis.

4 Discussion

Mean square displacement analysis is a powerful tool for the determination of dynamic parameters. It can be implemented in two different experimental ways: by computing it from trajectory data, recorded by single-particle tracking techniques, but also directly from images (iMSD), by studying fluorescence spatiotemporal correlation. By simulating image datasets, we studied systems of particles isotropically diffusing, concluding that both approaches are useful to study the particle's average motion, providing equivalent results (Fig. 3).

When computing MSD from tracking, it is necessary to record several trajectories, individually analyze each of them, and then average the outcomes to increase the statistical significance of the results. This can be experimentally challenging since it is time-consuming and it requires access to a large number of particles in appropriate conditions for tracking. On the other hand, iMSD provides equivalent averaged information from a single analysis of an image series. For many microscopes available in biophysics laboratories, imaging the region of interest can be more accessible than tracking single-particles. Additionally, this method ensures that every particle that contributes to the final results is measured in identical experimental conditions, which could be difficult to accomplish if multiple experiments are required to record enough trajectories. In regards to noise, iMSD can provide consistent results even in presence of Poissonian background noise of up to 20% of the particles' brightness.

We demonstrated that the equivalence between both approaches persists when the concentration is low, even if the system under study consists of one isolated particle (Fig. 4). This shows that iMSD can be used in a broader range of concentration scenarios than tracking and MSD since it is also applicable in systems where concentration would be too high to localize and track individual particles for long periods of time (Fig. 5).

In systems conformed by more than one species, single-particle tracking and MSD provides high specificity revealing individual aspects of motion that are hidden in the inherent averaging of fluctuation-based methods. However, we showed that iMSD can differentiate one and two-species situations, while providing complementary valuable information about them. We studied the case of two populations of free diffusing particles and showed that the anomalous parameter α can be associated with the ratio between the two different diffusion coefficients (Fig. 6).

5 Conclusions

In this work, we have presented a comprehensive discussion on the use of the mean square displacement (MSD) analysis computed from single-particle trajectories compared to those computed from optical images as a powerful tool to determine the laws of diffusion of moving particles.

In one-specie systems, we showed that both approaches provide equivalent averaged information. The iMSD analysis is also suitable for ultra-diluted samples even if the analysis is applied to isolated particles. In two-species systems, iMSD provides complementary information to that obtained by single-particle tracking techniques, characterizing the disparity between short and long-spatiotemporal scale behaviors.

These unique properties position iMSD as a fast and robust method, and an easy-to-apply alternative to tracking, opening new opportunities for studying intra-cellular dynamics using equipment commonly available in any biophysical laboratory.

Acknowledgments

This work was supported by the University of Buenos Aires (Grant # PIDAE 2019-3444 and PIDAE 2020-3980), the Sistema Nacional de Laseres (RESOL-2016-42-E-APN-SECACT#MCT) and ANPCyT (Grant #PICT 2020-02718).

Conflict of interest

The authors declare no conflict of interest.

Data availability statement

All data that support the findings of this study are included within the article (and any supplementary files).

References

[1] Ulrich Kubitscheck. *Fluorescence microscopy: from principles to biological applications*. John Wiley & Sons, 2017.

[2] Sviatlana Shashkova and Mark C. Leake. Single-molecule fluorescence microscopy review: shedding new light on old problems. *Bioscience Reports*, 37(4), 2017. BSR20170031.

[3] John SH Danial, Yasmine Aguib, and Magdi H Yacoub. Advanced fluorescence microscopy techniques for the life sciences. *Global Cardiology Science and Practice*, 2016(2), 2016.

[4] Feiran Huang, Erin Watson, Christopher Dempsey, and Junghae Suh. *Real-Time Particle Tracking for Studying Intracellular Trafficking of Pharmaceutical Nanocarriers*, pages 211–223. Humana Press, Totowa, NJ, 2013.

[5] Beth L. Haas, Jyl S. Matson, Victor J. DiRita, and Julie S. Biteen. Single-molecule tracking in live *Vibrio cholerae* reveals that ToxR recruits the membrane-bound virulence regulator TcpP to the toxT promoter. *Molecular Microbiology*, 96(1):4–13, November 2014.

[6] Rhonda J. Davey, Michelle A. Digman, Enrico Gratton, and Pierre D. J. Moens. Quantitative image mean squared displacement (iMSD) analysis of the dynamics of profilin 1 at the membrane of live cells. *Methods*, 140-141:119–125, May 2018.

[7] Hellen C. Ishikawa-Ankerhold, Richard Ankerhold, and Gregor P. C. Drummen. Advanced fluorescence microscopy techniques—FRAP, FLIP, FLAP, FRET and FLIM. *Molecules*, 17(4):4047–4132, April 2012.

[8] Michael J. Saxton and Ken Jacobson. Single-particle tracking: Applications to membrane dynamics. *Annual Review of Biophysics and Biomolecular Structure*, 26(1):373–399, June 1997.

[9] Benedict Hebert, Santiago Costantino, and Paul W. Wiseman. Spatiotemporal image correlation spectroscopy (STICS) theory, verification, and application to protein velocity mapping in living CHO cells. *Biophysical Journal*, 88(5):3601–3614, May 2005.

[10] Carmine Di Rienzo, Enrico Gratton, Fabio Beltram, and Francesco Cardarelli. Fast spatiotemporal correlation spectroscopy to determine protein lateral diffusion laws in live cell membranes. *Proceedings of the National Academy of Sciences*, 110(30):12307–12312, July 2013.

[11] Carmine Di Rienzo, Vincenzo Piazza, Enrico Gratton, Fabio Beltram, and Francesco Cardarelli. Probing short-range protein brownian motion in the cytoplasm of living cells. *Nature Communications*, 5(1), 2014.

[12] Luca Digiacomo, Michelle A. Digman, Enrico Gratton, and Giulio Caracciolo. Development of an image mean square displacement (iMSD)-based method as a novel approach to study the intracellular trafficking of nanoparticles. *Acta Biomaterialia*, 42:189–198, September 2016.

[13] Luca Digiacomo, Francesca D'Autilia, William Durso, Paolo Maria Tentori, Giulio Caracciolo, and Francesco Cardarelli. Dynamic fingerprinting of sub-cellular nanostructures by image mean square displacement analysis. *Scientific Reports*, 7(1):14836, November 2017.

[14] Leonel Malacrida, Estella Rao, and Enrico Gratton. Comparison between iMSD and 2d-pCF analysis for molecular motion studies on in vivo cells: The case of the epidermal growth factor receptor. *Methods*, 140–141:74–84, May 2018.

[15] David J. Rowland, Hannah H. Tuson, and Julie S. Biteen. Resolving fast, confined diffusion in bacteria with image correlation spectroscopy. *Biophysical Journal*, 110(10):2241–2251, May 2016.

[16] Gianmarco Ferri, Luca Digiacomo, Francesca D'Autilia, William Durso, Giulio Caracciolo, and Francesco Cardarelli. Time-lapse confocal imaging datasets to assess structural and dynamic properties of subcellular nanostructures. *Scientific Data*, 5:180191, September 2018.

[17] Giulia Tedeschi, Lorenzo Scipioni, Maria Papanikolaou, Geoffrey W. Abbott, and Michelle A. Digman. Fluorescence fluctuation spectroscopy enables quantification of potassium channel subunit dynamics and stoichiometry. *Scientific Reports*, 11(1):10719, May 2021.

[18] A. Kusumi, Y. Sako, and M. Yamamoto. Confined lateral diffusion of membrane receptors as studied by single particle tracking (nanovid microscopy). effects of calcium-induced differentiation in cultured epithelial cells. *Biophysical Journal*, 65(5):2021–2040, November 1993.

[19] M.J. Saxton. Single-particle tracking: the distribution of diffusion coefficients. *Biophysical Journal*, 72(4):1744–1753, April 1997.

[20] Dominique Ernst and Jürgen Köhler. Measuring a diffusion coefficient by single-particle tracking: statistical analysis of experimental mean squared displacement curves. *Phys. Chem. Chem. Phys.*, 15(3):845–849, 2013.

[21] D. Sage, F.R. Neumann, F. Hediger, S.M. Gasser, and M. Unser. Automatic tracking of individual fluorescence particles: application to the study of chromosome dynamics. *IEEE Transactions on Image Processing*, 14(9):1372–1383, September 2005.